Journal of Medicinal Chemistry

Article

pubs.acs.org/jmc

In Vitro Evaluation of the Interaction of Dextrin−Colistin Conjugates with Bacterial Lipopolysaccharide

Jessica L. Roberts,[†,⊥] Beatrice Cattoz,[‡] Ralf Schweins,[§] Konrad Beck,[†] David W. Thomas,[†] Peter C. Griffiths,[‡] and Elaine L. Ferguson*[,†]

[†]Advanced Therapies Group, School of Dentistry, Cardiff University, Heath Park, Cardiff CF14 4XY, U.K.

[‡]Department of Pharmaceutical, Chemical and Environmental Sciences, Faculty of Engineering and Science, University of Greenwich, Medway Campus, Central Avenue, Chatham Maritime ME4 4TB, U.K.

[§]Institut Laue-Langevin, DS/LSS group, 6, rue Jules Horowitz, 38042 Cedex 9 Grenoble, France

Supporting Information

ABSTRACT: Dextrin−colistin conjugates have been developed with the aim of achieving reduced clinical toxicity associated with colistin, also known as polymyxin E, and improved targeting to sites of bacterial infection. This study investigated the in vitro ability of such dextrin−colistin conjugates to bind and modulate bacterial lipopolysaccharide (LPS), and how this binding affects its biological activity. These results showed that colistin and amylase-activated dextrin−colistin conjugate to a lesser extent induced aggregation of LPS to form a stacked bilayer structure with characteristic dimensions, although this did not cause any substantial change in its secondary structure. In biological studies, both colistin and dextrin−colistin conjugate effectively inhibited LPS-induced hemolysis and tumor necrosis factor α (TNFα) secretion in a concentration-dependent manner, but only dextrin−colistin conjugate showed no additive toxicity at higher concentrations. This study provides the first direct structural experimental evidence for the binding of dextrin−colistin conjugates and LPS and gives insight into the mode of action of dextrin−colistin conjugates.

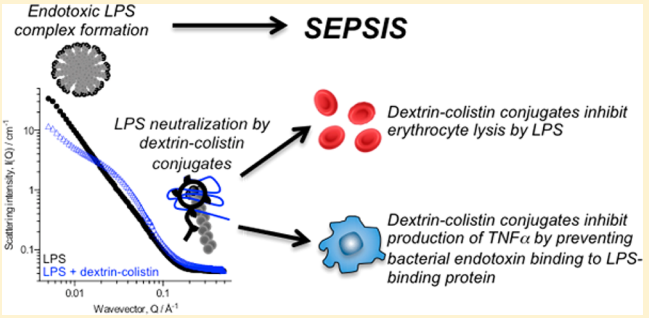

INTRODUCTION

Infectious diseases account for millions of deaths worldwide annually with high associated costs.[1] Antibiotic chemotherapy is successfully used to treat the majority of Gram-negative infections, but antibiotic-induced shedding of endotoxic lipopolysaccharides (LPSs) may result in systemic sepsis, with an associated mortality of 30−50%. Thus, eradication of bacterial infection does not always lead to a positive clinical outcome. We have previously described the first bioresponsive polymer conjugates to target the delivery of antimicrobials to sites of inflammation, using dextrin−colistin conjugates as a prototypical model.[2] Colistin (also known as polymyxin E) is an effective amphiphilic antibiotic that binds to Gram-negative bacterial cell membranes, resulting in cytoplasmic leakage and cell death. In clinical use, however, colistin may be associated with considerable nephro- and neurotoxicity in immunocompromized patients, which limits its clinical use. These nanoantibiotic polymer therapeutics are administered centrally but are locally activated at sites of infection by amylase, an enzyme found throughout the body (typical serum concentration 60−120 IU/L) but present at elevated concentrations at sites of infection or inflammation.[3] This local activation improves antibiotic targeting to sites of infection, enables the unmasking and localized release of free colistin (using polymer masked−unmasked protein therapy (PUMPT)),[4] and reduces clinical toxicity.

An important property of colistin is its ability to bind bacterial LPS and block its toxic biological activities[5] (Figure 1). The phase structure, conformation, and aggregation behavior of bacterial LPS and its components (e.g., lipid A) have been extensively characterized by various physical methods.[6−8] LPS is biologically active in its micellar form, and colistin disaggregation effectively neutralizes its endotoxic effects by disrupting the regular spacing of LPS fatty acid chains and binding in a 1:1 complex.[9] While the toxicity profile and antibacterial activity of the dextrin−colistin conjugates have been described, its potential structural and functional interactions with LPS are unknown. In these studies, colistin−LPS complex formation and potential LPS neutralization was studied using small-angle neutron scattering (SANS), circular dichroism (CD) spectroscopy, and turbidity assays to characterize the in vitro ability of the conjugates to bind and modulate bacterial LPS from *Escherichia coli* and determine how the degree of unmasking affected LPS binding. Parallel studies investigated in vitro inhibition of LPS-induced erythrocyte hemolysis and tumor necrosis factor α

Received: September 30, 2015
Published: January 5, 2016

DOI: 10.1021/acs.jmedchem.5b01521
J. Med. Chem. 2016, 59, 647−654

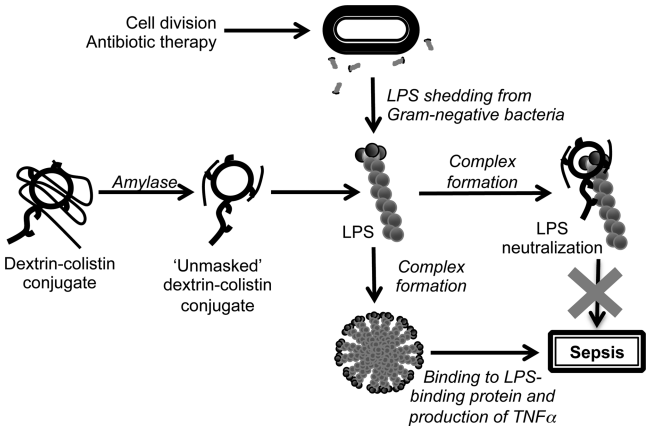

Figure 1. Representation of the antiendotoxin mechanism of dextrin−colistin conjugate, showing the unmasking strategy utilized to control delivery of colistin and the effect of colistin on LPS aggregates.

(TNFα) release from human kidney (HK-2) cells as a marker of LPS complex formation with colistin sulfate, colistimethate sodium (CMS), and dextrin−colistin conjugate.

RESULTS

Endotoxin Binding. In SANS experiments, LPS aggregates showed significant scattering intensity, $I(Q)$ as a function of the wavevector, Q. This scattering is characteristic of the size, shape, and distribution of the scattering centers within the system under investigation. Clearly, the pattern was altered in the presence of colistin or unmasked dextrin−colistin conjugate at ≥10 mg/mL (Figure 2). The emergence of two peaks at $Q = 0.06$ and 0.11 Å^{-1} and a pronounced increase in scattering intensity at low Q was apparent when LPS was combined with colistin. These peaks did not change position with different colistin concentrations, although the intensity of the peaks varied and was greatest with 10 mg/mL colistin. When LPS was preincubated with dextrin−colistin conjugate, the intensity decreased at low Q. Preincubation of dextrin−colistin conjugate with amylase, however, induced a time-dependent increase in scattering intensity at low Q and the appearance of a peak at Q = 0.06 Å^{-1}. Clearly the peaks are a result of the action of the colistin on the LPS structure.

When aggregation or association is induced in a sample at constant weight concentration, the scattering intensity reflects the changing distribution of scatterers within the system and, as such, is a complex interplay between the size and shape of the aggregated form

$$I(Q) = n_p V_p^2 P(Q) S(Q) + B_{inc}$$

where n_p is the number concentration of the scatterers, V_p is their volume, and $P(Q)$ and $S(Q)$ are mathematical functions that describe their shape and distribution. Hence, for a fixed mass concentration, aggregation leads to a decrease in n_p but an increase in V_p, as well as changes in $P(Q)$ and $S(Q)$. Here, the scattering is dominated by the LPSs, such that at low Q values, a shape-independent $P(Q)$ approach may be invoked ($P(Q) \rightarrow 1$, $S(Q) \rightarrow 1$), where $I(Q) \propto \exp[(QR_g)^2/3]$. Hence, a plot of ln $I(Q)$ vs Q^2 (a Guinier plot) will be linear, with slope $R_g^2/3$; a steep slope indicates a large size. An example of a Guinier plot is presented in the Supporting Information, and the R_g values are presented in Figure 2c. R_g is greatest for the LPS with colistin sulfate structure and smallest for the structure formed by LPSs in the presence of the masked dextrin−colistin conjugate. Interestingly, the structure of LPSs with masked dextrin−colistin conjugate is smaller than that of LPSs only, indicating that the masked conjugate must disrupt the LPS structure somewhat. Upon addition of colistin sulfate at 10 mg/mL, aggregation is induced leading to larger structures (steeper decay) and the emergence of the peaks indicating a stacked structure with characteristic dimensions L = 50 Å, with the second peak arising due to the second order reflection. The unmasked conjugate was seen to have little effect on the LPS structure. At the higher colistin concentration (50 mg/mL), the perturbation induced by the colistin is much greater with the signature of the stacked layers also emerging with the unmasked conjugates. At both conjugate concentrations, there is a downturn at low Q, indicating slightly smaller structures.

CD spectra recorded from 260 to ∼180 nm mainly reflect the conformation of the colistin peptide bonds (Figure 3a−c). The pronounced minimum at 198 nm is indicative of a random coil conformation though the shoulder in the 215−225 nm range reflects some ordered structures. Neither conjugation with dextrin (Figure 3b) nor subsequent unmasking by amylase (Figure 3c) showed any effect on the peptide conformation. Succinoylated dextrin showed no CD signal within the accessible wavelength range (data not shown). When LPS was added to the antibiotic solutions, the CD spectra appeared to be equivalent to the sum of the CD signals of the individual components.

Increasing turbidity was used as a marker of LPS aggregate formation with colistin, CMS, or dextrin−colistin conjugate. When compared at equivalent colistin concentration, significant differences between the turbidity of colistin and CMS, dextrin−colistin (with or without amylase), or control were observed (Figure 3d). LPS binding of the dextrin−colistin conjugate was reduced to ∼50% compared with free colistin; turbidity remained unaltered even after preincubation of the conjugate with amylase.

Colistin and CMS to a lesser extent were able to inhibit the cleavage of chromogenic substrate by LPSs (Figure 4). Neutralization of LPS by colistin required 20-fold more LPSs to trigger *Limulus* amebocyte lysate (LAL) gelation compared with LPSs in water and was significantly greater than that with CMS (1 vs 0.05 ng/mL, respectively). All dextrin−colistin conjugate samples gelled *Limulus* amebocyte lysate without the addition of LPSs. Nevertheless, at the lower concentrations of LPSs, unmasked conjugate was capable of binding more LPSs than masked conjugate, and there was a trend for increasing endotoxin binding after unmasking by amylase (6 h > 24 h > 0 h) (data not shown).

In Vitro Inhibition of Endotoxin Activity. When HK-2 cells were treated with LPSs alone or in the presence of colistin sulfate, CMS, or unmasked dextrin−colistin conjugate, there was little effect on LPS-induced TNFα release at low concentrations, but increased cytokine release was observed when colistin molar concentration exceeded that of LPSs (Figure 5). However, at both LPS concentrations (10 and 100 ng/mL), dextrin−colistin conjugate inhibited LPS-induced TNFα release in a concentration-dependent manner above 5 and 50 μg/mL, respectively.

Similarly, addition of colistin sulfate, CMS, and dextrin−colistin conjugate inhibited endotoxin-induced hemolysis of rat erythrocytes up to ∼20 μg/mL (Figure 6). However, while higher concentrations of colistin and CMS caused increasing erythrocyte lysis, dextrin−colistin conjugate continued to inhibit hemolysis in a concentration-dependent manner. Unmasked dextrin−colistin conjugate was unable to inhibit endotoxin-

DOI: 10.1021/acs.jmedchem.5b01521
J. Med. Chem. 2016, 59, 647−654

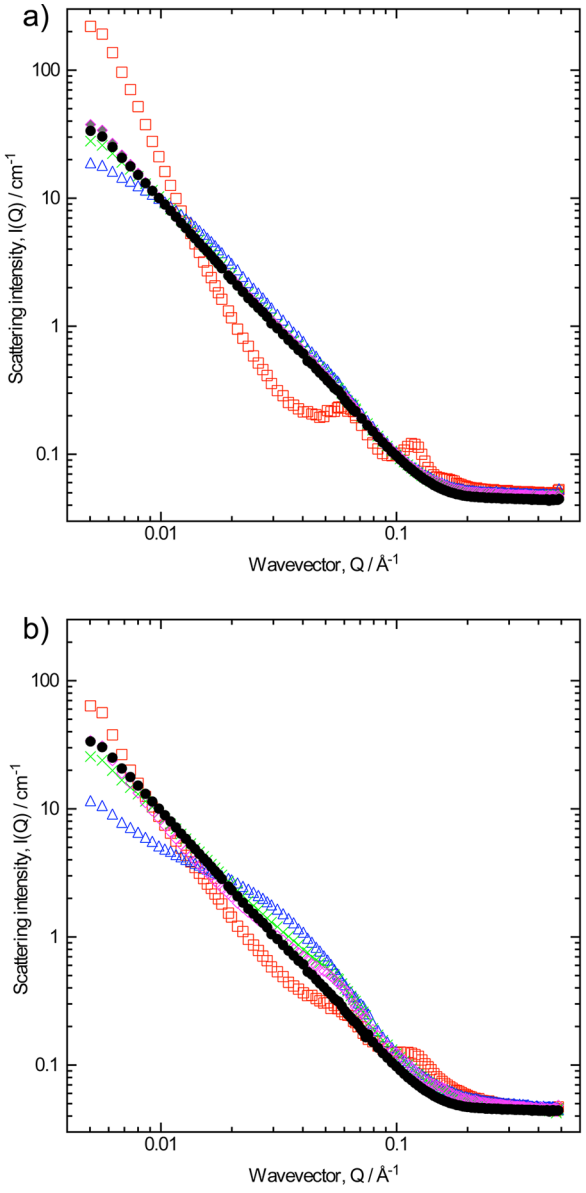

c)

Sample	R_g at 10 mg/mL (Å)	R_g at 50 mg/mL (Å)
□ LPS + colistin	329	305
△ LPS + dextrin-colistin	169	188
× LPS + 6 h unmasked dextrin-colistin	213	215
◇ LPS + 24 h unmasked dextrin-colistin	244	253
● LPS	233	

Figure 2. Small-angle neutron scattering from LPS (10 mg/mL in D_2O) following incubation (3 h at 37 °C) with colistin sulfate, dextrin−colistin conjugate, and unmasked dextrin−colistin conjugates at (a) 10 and (b) 50 mg/mL. Panel c shows the radii of gyration (R_g) calculated from the SANS data.

induced hemolysis and caused equivalent toxicity to colistin and CMS at higher concentrations.

DISCUSSION

A detailed understanding of the physicochemical properties and structure−activity relationships is vital to predict the behavior of polymer therapeutics in biological systems and ensure the design of safe and efficacious nanomedicines. The ability of colistin to bind and neutralize LPS is well documented; however little is known about how polymer conjugation affects the structural and biological properties of colistin. While the antimicrobial activity of dextrin−colistin conjugates has been demonstrated in vitro,[2] antibiotic treatment may induce LPS release from lysed bacteria, which may trigger the immune system to induce endotoxic shock. Therefore, these studies investigated whether dextrin−colistin conjugates (before and after amylase "unmasking") could

DOI: 10.1021/acs.jmedchem.5b01521
J. Med. Chem. 2016, 59, 647−654

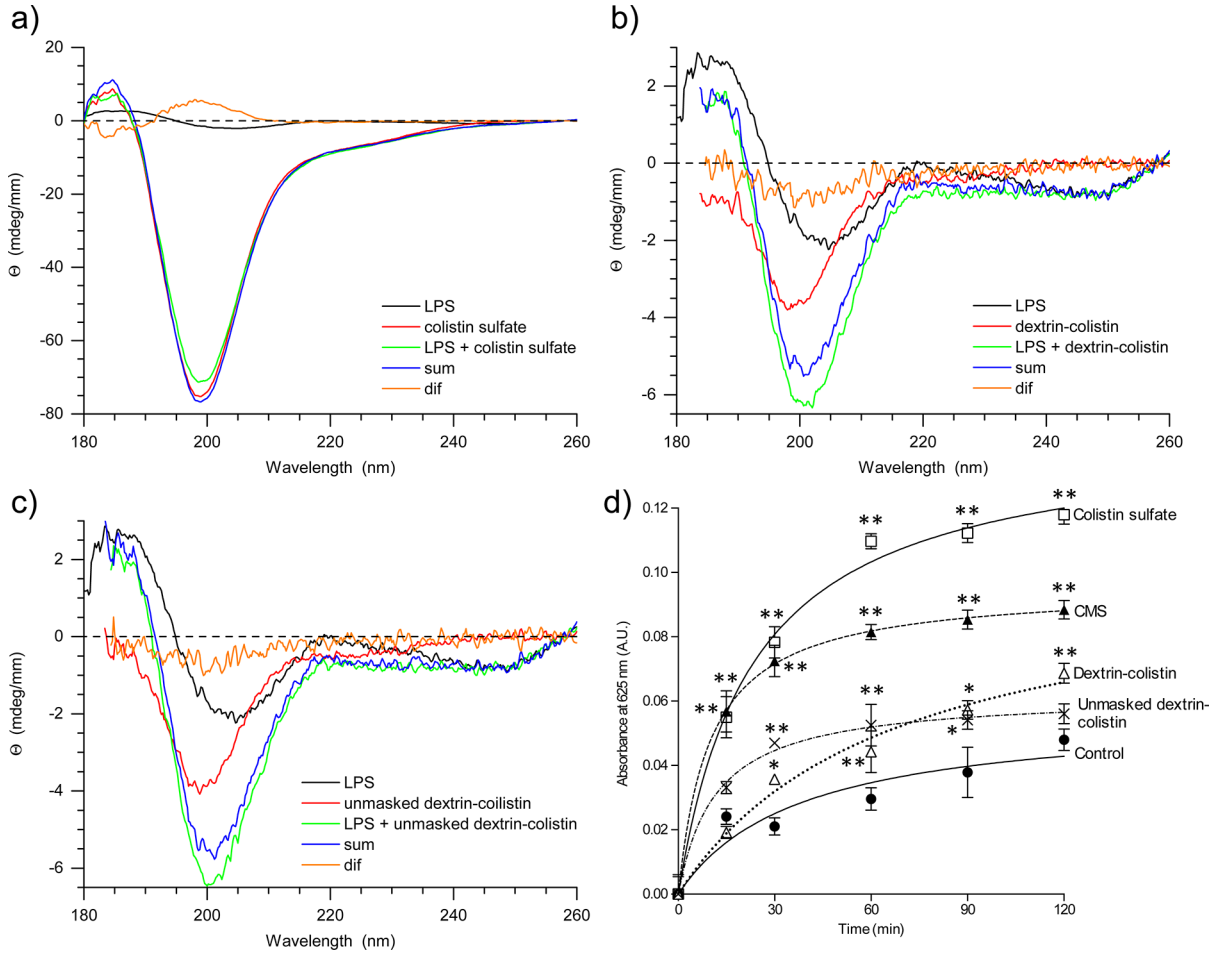

Figure 3. CD spectra of (a) colistin sulfate, (b) dextrin−colistin conjugate, and (c) unmasked dextrin−colistin conjugate (0.5 mg/mL) in 100 mM NaF, 20 mM KH_2PO_4, pH 7.4, and following incubation (3 h at 37 °C) with LPS (0.1 mg/mL), where sum = LPS signal + colistin signal and dif = LPS−colistin mixture signal − sum. Panel d shows precipitation of LPS from *E. coli* (1 mg/mL) in the absence and presence of colistin sulfate, CMS, dextrin−colistin conjugate, and unmasked dextrin−colistin conjugate (4 mg/mL colistin equiv). Data represent mean ± SEM, $n = 6$; $^*p < 0.01$ and $^{**}p < 0.001$ indicate significance compared with LPS alone (control).

bind and neutralize released endotoxins. Dextrin−colistin conjugates used in these studies contained ∼10% w/w colistin, of which <2% was unbound, indicating multiple (typically two) dextrin chains per colistin with several (typically three) binding sites. The dextrin−colistin concentrations used in the SANS and CD spectroscopy studies refer to total conjugate; thus conjugate samples contained ∼10× less colistin than the equivalent free drug samples. While this may affect the biological activity of the conjugates, it was deemed the most appropriate means of comparing the samples in these structural studies.

The use of SANS to study evolving biological systems has been previously employed to investigate dextrin−phospholipase A_2-triggered degradation of liposomes.[10] Here, we examined the effect of dextrin conjugation and unmasking by amylase on the interaction of colistin with LPSs. With a critical micelle concentration of ∼14 μg/mL,[8,11] LPSs readily micellize at the concentrations used in these studies. These studies assumed, not unreasonably, that the SANS scattering is dominated by that of the LPSs. The data revealed significant conformational rearrangement of LPSs following incubation with both colistin sulfate and unmasked dextrin−colistin conjugate (colistin sulfate > 24 h unmasked dextrin−colistin > 6 h unmasked dextrin−colistin) at ≥10 mg/mL. This conformational rearrangement was evident in the emergence of the peaks indicative of a regular ordered structure.

Similarly, marked differences between the aggregation of colistin and LPSs and that observed with dextrin−colistin conjugates were evident in both the turbidity and LAL assays. The CD spectra of colistin sulfate were in agreement with the solution structure derived by nuclear magnetic resonance (NMR) spectroscopy,[9] showing overall high mobility but some β-turn formed by residues 5−8. However, CD spectroscopy did not show any substantial change in the secondary structure of colistin or dextrin−colistin conjugates (masked and unmasked) in the presence of LPS, indicating that this aggregation did not induce an α-helical structure, presumably due to the rigidity of colistin's cyclic structure. This has also been observed with polymyxin B, while WLBU2, a cationic amphiphilic peptide, became markedly helical in the presence of LPSs, a finding attributed to the ability of polymyxin B (but not WLBU2) to destabilize and disrupt LPS vesicles.[12]

Molecular modeling has demonstrated that colistin exerts its antiendotoxic effects by breaking up the supramolecular structure of LPSs.[9] The downturn in the SANS from LPSs at low Q in the presence of colistin (50 mg/mL) is an indication of this neutralization effect, since LPSs and colistin have been shown to bind at a LPS to colistin ratio of 5.2:1 (by weight).[13]

DOI: 10.1021/acs.jmedchem.5b01521
J. Med. Chem. 2016, 59, 647−654

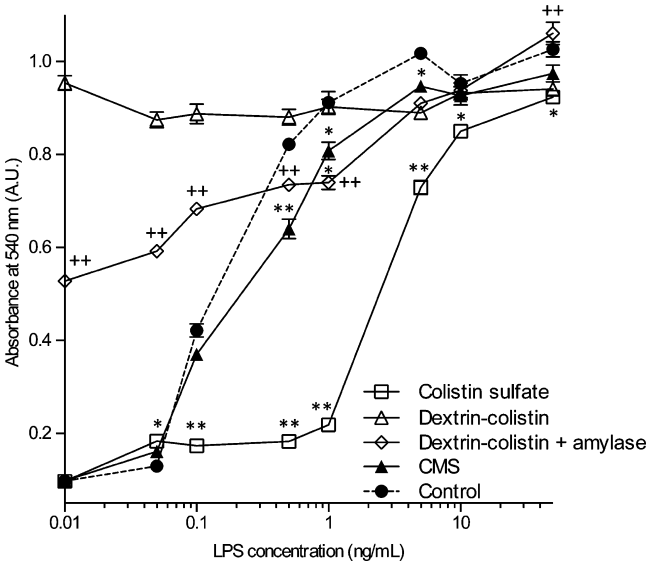

Figure 4. Colorimetric detection of endotoxin following incubation of LAL with LPS from *E. coli* (0−50 ng/mL) in pyrogen-free water or preincubated for 3 h at 37 °C with colistin sulfate, CMS, dextrin−colistin conjugate, and unmasked dextrin−colistin conjugate (4 μg/mL colistin equiv). Data represent the mean ± SEM, $n = 6$; *$p < 0.01$ and **$p < 0.001$ indicate significance compared with LPS alone (control); ++ ($p > 0.001$) indicates significance compared with dextrin−colistin conjugate.

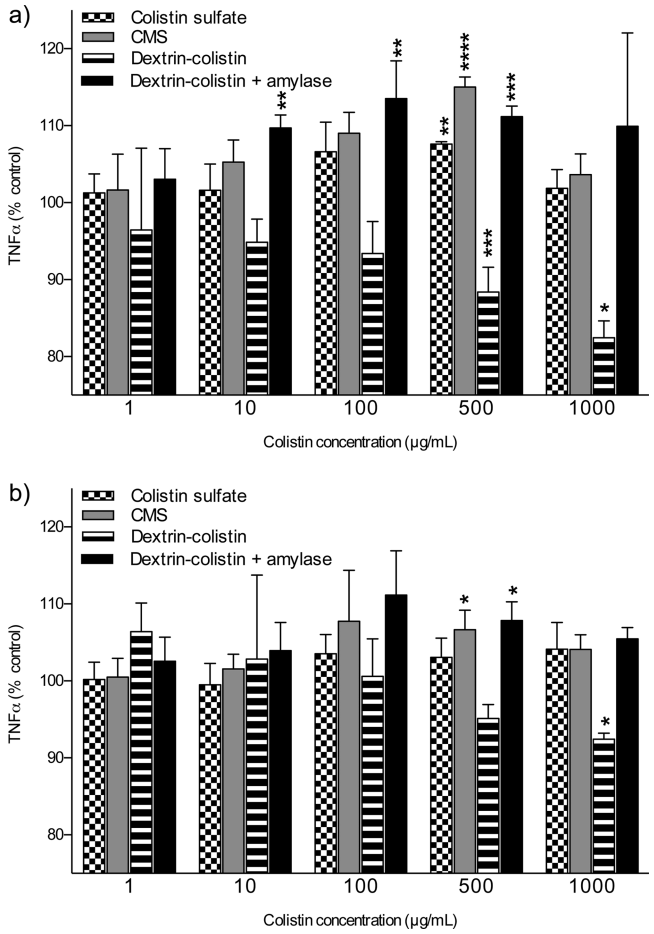

Figure 5. Inhibition of LPS-induced TNFα release from HK-2 cells following incubation with colistin sulfate, CMS, dextrin−colistin conjugate, and dextrin−colistin + amylase at 0.1−1000 μg/mL colistin equiv (24 h incubation). Panels a and b show cell response to 10 and 100 ng/mL LPS, respectively. Data represents mean percentage TNFα release ± SD, $n = 3$; *$p < 0.05$, **$p < 0.01$, ***$p < 0.001$, and ****$p < 0.0001$ indicate significance compared with LPS alone (control).

The regularity and clarity of the peaks in the SANS induced by colistin are commensurate with a spacing of 5 nm, suggestive of a bilayer stack. The 5 nm structures seen here are in good agreement with the reported size of the lipid A bilayer component of bacterial LPS, described in both SANS[6] and molecular modeling and X-ray powder diffraction experiments.[14] These studies demonstrated that lipid A and rough LPS (having a short O-specific chain, like *E. coli* O26:B6 used here) are 2.4 and 2.8 nm long, respectively. This would indicate that the structures seen in these studies are from the LPSs. This is further supported by Wallace et al.,[15] who reported that colistin aggregates formed above 2.1 μg/mL with a diameter of 2.07 ± 0.3 nm.

Binding and structural data using several biophysical techniques, including isothermal titration calorimetry, fluorescent probes, and NMR spectroscopy, have indicated that the LPS−colistin interaction is a two-stage mechanism.[16] First, the complex is stabilized by electrostatic charges between colistin's positive charges and LPS's negatively charged head groups. Subsequently, complexation is strengthened by hydrophobic interactions between the hydrophobic domains of the two molecules. Given that dextrin−colistin conjugation uses approximately three of colistin's positively charged amine groups, it is unsurprising that masked conjugates have no effect on LPS structure. While unmasked conjugates induced some conformational rearrangement of LPS, this was not as obvious as with native colistin. This was not surprising since α-amylase is an endoamylase that cleaves dextrin within the polyglucose chain; thus, unmasked dextrin−colistin conjugates retain oligosaccharide fragments attached to colistin's amine groups, which would reduce its cationic charge.

Parallel studies investigated in vitro inhibition of LPS-induced erythrocyte lysis and TNFα release from human kidney cells as a marker of LPS aggregate formation with colistin or dextrin−colistin conjugate. Following systemic administration, dextrin−colistin conjugates are expected to remain in the bloodstream for an extended period, due to their macromolecular size, but would ultimately be excreted via the kidneys following amylase unmasking. Despite the negligible binding to bacterial LPS, the ability of dextrin−colistin conjugates to exert a protective effect from endotoxins on erythrocytes and human kidney cells was in keeping with previous studies showing that dextrin is able to effectively impede the hemolytic activity of drugs, such as zidovudine,[17] and proteins, such as phospholipase A_2.[18] In these previous studies, the effect was evident when zidovudine was covalently linked to dextrin or physically mixed with dextrin, providing further proof that dextrin acts by a cytoprotective mechanism. Moreover, iodine−lithium−α-dextrin conjugates have been described with antiendotoxin activity.[19,20] These studies demonstrated that iodine−lithium−α-dextrin suppresses CD14 receptor expression, inhibits LPS-induced pro-inflammatory activation of monocytes and neutrophils, and increases tolerance to endotoxins.

Polymyxin B−dextran 70 conjugates have been described that effectively inhibit LPS-induced TNFα production in vivo. Lake et al.[21] proposed that polymyxin B−dextran 70 conjugates neutralize the pathogenic pharmacophore of endotoxin, citing unpublished studies corroborating its ability to bind to radiolabeled endotoxin. Interestingly, parallel studies reported markedly reduced antibiotic activity of dextran−polymyxin B

DOI: 10.1021/acs.jmedchem.5b01521
J. Med. Chem. 2016, 59, 647−654

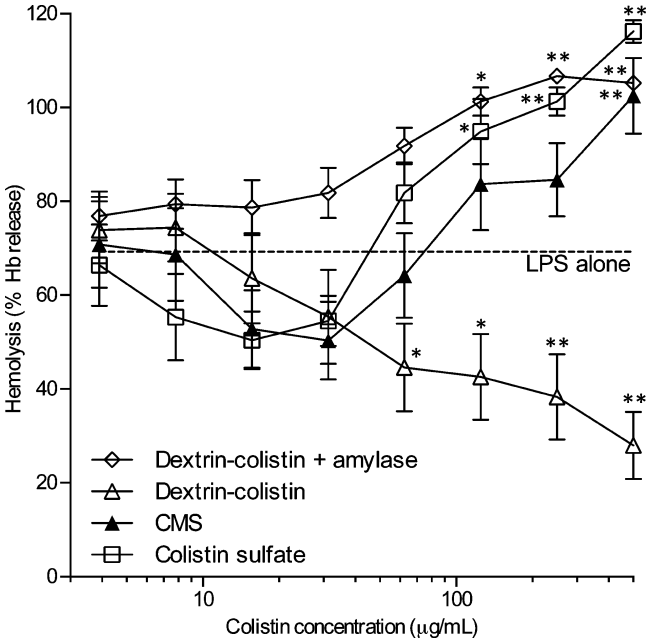

Figure 6. Inhibition of LPS-induced (100 μg/mL) hemolysis (24 h incubation) of rat erythrocytes following preincubation with colistin sulfate, CMS, dextrin–colistin conjugate, and unmasked dextrin–colistin conjugate for 3 h at 37 °C. Data represents mean ± SEM, $n = 9$; *$p < 0.05$ and **$p < 0.001$ indicate significance compared with LPS alone (control).

conjugates containing 70 000 g/mol dextran and 3.8% w/w polymyxin B (equivalent to 2.1 polymyxin B per dextran).[22] In contrast, our dextrin–colistin conjugates contain 8000 g/mol dextrin and 10.1% w/w colistin, equivalent to 1.6 dextrin chains per colistin, which may explain the difference in antibacterial activity.

CONCLUSIONS

These data demonstrate physical differences in the LPS interaction of colistin and dextrin–colistin conjugates pre- and postamylase unmasking. No change in the LPS structure was observed for dextrin–colistin conjugates; however, degradation of conjugates showed time-dependent changes in LPS complex formation that were more pronounced after prolonged incubation with amylase. Despite the inability of dextrin–colistin conjugates to bind to bacterial LPS, concentration-dependent inhibition of LPS-induced toxicity was evident, indicating that dextrin–colistin conjugates could represent effective neutralizers of endotoxin with application in the treatment of sepsis.

EXPERIMENTAL SECTION

Dextrin–Colistin Conjugate Synthesis and Unmasking. Dextrin–colistin conjugate was synthesized, using 1-ethyl-3-(3-dimethylaminopropyl)carbodiimide hydrochloride and *N*-hydroxysulfosuccinimide and characterized as previously described.[2] The dextrin–colistin conjugate used in these studies contained dextrin with 1.1 mol % succinoylation and had a molecular weight of approximately 9000 g/mol (gel permeation chromatography with pullulan standards) and a colistin content of approximately 10.1% w/w (by bicinchoninic acid assay) with <3% free colistin (by fast protein liquid chromatography). Purity of dextrin–colistin conjugates was ≥95% (by gel permeation chromatography). If not stated otherwise, unmasked dextrin–colistin conjugates were prepared by incubation of dextrin–colistin conjugate (10 mg/mL) with amylase (100 IU/L) for 24 h at 37 °C.

Small-Angle Neutron Scattering Measurements. To assess the colistin-induced disruption of LPS aggregates, LPS from *E. coli* 026:B6 (5) (10 mg/mL; Sigma-Aldrich, U.K.) was incubated with succinoylated dextrin, colistin sulfate (Sigma-Aldrich, U.K.), dextrin–colistin conjugate, or unmasked dextrin–colistin conjugate (0.01, 0.1, 1, 10, or 50 mg/mL) in deuterium oxide (D_2O) (Sigma-Aldrich, U.K.) containing phosphate buffered saline (PBS, 137 mM NaCl, 3 mM KCl, 8 mM Na_2HPO_4, 1.5 mM KH_2PO_4, pH 7.3 (Oxoid, U.K.), 3 h at 37 °C, pH 7.4) prior to analysis by SANS. Unmasked dextrin–colistin conjugates were prepared by incubation of dextrin–colistin conjugate (50 mg/mL in PBS) with α-amylase from human saliva (100 IU/L) (Sigma-Aldrich, U.K.) for 6 or 24 h at 37 °C, then lyophilized and stored at −20 °C before reconstitution in D_2O prior to analysis by SANS.

SANS experiments were performed on the steady-state reactor source on the D22 diffractometer at the ILL, Grenoble. A $Q = (4\pi/\lambda)\sin(\theta/2)$ range between 0.005 and 0.5 Å^{-1} was obtained by choosing two instrument settings at a constant neutron wavelength (λ) of 6 Å, the two sample–detector distances were 2 and 14 m, respectively, both working with the detector being offset by 40 cm with respect to the direct beam position on the detector. The samples were contained in 2 mm path length, UV-spectrophotometer grade, quartz cuvettes (Hellma, U.K.). All experiments were conducted at 37 °C.

All scattering data were (a) normalized for the sample transmission, (b) background corrected using a quartz cell filled with PBS in D_2O, and (c) corrected for the linearity and efficiency of the detector response using the instrument specific software package. Data was analyzed using SasView 2.2.0 software.

Circular Dichroism Spectroscopy. CD spectra were acquired on a model 215 spectrometer (AVIV Instrument Inc., Lakewood, NJ) with a 1 mm path length quartz cell at 4 °C. Spectra were recorded at 0.2 nm intervals with 3 s/point at a 1 nm bandwidth with the dynode voltage < 500 V, and buffer baselines were subtracted. Samples were dissolved in 100 mM NaF, 20 mM KH_2PO_4/NaOH, pH 7.4. Spectra of succinoylated dextrin, colistin sulfate, dextrin–colistin conjugate, or unmasked dextrin–colistin conjugate (0.5 mg/mL) were obtained alone and following incubation with LPS (0.1 mg/mL; 3 h at 37 °C). Experiments were performed once.

Turbidity Assay. A turbidimetric assay technique was used in which the binding of LPS to colistin results in precipitation of aggregates and increased turbidity. LPS was dissolved in prewarmed PBS (1 mg/mL, 37 °C, pH 7.4) containing colistin sulfate, CMS (Colomycin injection, Forest Laboratories UK Limited, U.K.), dextrin–colistin conjugate, or unmasked dextrin–colistin conjugate (4 mg/mL colistin equiv, 200 μL per well) and added to the wells of a 96-well microtiter plate. Control samples contained only LPS dissolved in PBS. Plates were incubated at 37 °C throughout the experiment, and absorbance was read at 625 nm at various time points. Samples were assayed in triplicate and experiments were repeated once.

***Limulus* Amebocyte Lysate (LAL) Assay.** Endotoxin neutralization was evaluated using a ToxinSensor chromogenic LAL endotoxin assay kit (GenScript, U.S.A.). LPS was dissolved in pyrogen free water (0–50 ng/mL) containing colistin sulfate, CMS, dextrin–colistin conjugate, or unmasked dextrin–colistin conjugate (4 μg/mL colistin equiv, 100 μL) in pyrogen-free vials. Control samples contained only LPS dissolved in pyrogen-free water. Solutions were mixed well and incubated at 37 °C for 3 h. The manufacturers' test procedure for quantitative detection of endotoxins was then followed. The concentration of LPS producing 50% maximal absorption was taken as the ED_{50}. Experiments were performed once with six repeated measures for each concentration.

Unmasked dextrin–colistin conjugates were prepared by incubation of dextrin–colistin conjugate (0.5 mg/mL in pyrogen free water) with amylase from human saliva (100 IU/L) for 6 h at 37 °C. The LAL assay was then followed as described above.

Cell Culture. An immortalized proximal tubule epithelial cell line from normal human kidney (HK-2, ATCC CRL-2190) was cultured in keratinocyte-serum free medium (K-SFM) (Invitrogen Life Technologies, U.K.).

Expression of TNFα. HK-2 cells were seeded into sterile 96-well microtiter plates (2×10^5 cells/mL) in 0.1 mL/well media and allowed

DOI: 10.1021/acs.jmedchem.5b01521
J. Med. Chem. 2016, 59, 647–654

to adhere for 24 h. The medium was then removed and LPS (10 ng/mL) was added in the absence or presence of colistin sulfate, CMS, or dextrin−colistin conjugate (with or without amylase, 100 IU/L; 0.2 μm filter-sterilized) at different concentrations. After 24 h, microtiter plates were centrifuged (600*g*, 10 min), and the supernatant was transferred to a clean 96-well plate and stored at −20 °C until determination of TNFα content using a commercial human TNFα ELISA set (Thermo Scientific, U.K.) according to the manufacturer's protocol. Absorbance was measured at 450 nm using a microtiter plate reader. The absorbance values were expressed as mean ± SD (n = 3) and used to calculate TNFα concentration in pg/mL (assay detection range 15−1000 pg/mL). All experiments were performed three times for each concentration.

Erythrocyte Lysis. A rat erythrocyte suspension were prepared as previously described[18] and was added to a preincubated (3 h, 37 °C) 96-well plate containing LPS (100 μg/mL final concentration) in the presence of colistin sulfate, CMS, dextrin−colistin conjugate, or unmasked dextrin−colistin conjugate (0−500 μg/mL colistin equiv final concentration, 200 μL final well volume). PBS was used as a negative control, and Triton X-100 (1% v/v; Sigma-Aldrich, U.K.) was used to achieve 100% hemolysis. The plate was incubated for 24 h at 37 °C and then centrifuged at 1500*g* for 10 min at 4 °C. The supernatant (100 μL) of each well was then carefully removed and placed into a clean 96-well plate, and absorbance at 540 nm was read. The background hemolysis (PBS) was subtracted, and the results were expressed as percentage hemoglobin released (±SEM). Unmasked dextrin−colistin conjugates were prepared by incubation of dextrin−colistin conjugate (2 mg/mL in PBS) with amylase (100 IU/L) for 24 h at 37 °C. All experiments were replicated three times with triplicate repeated measures within each replication for each concentration.

Statistics. The significance of the data was assessed using one-way analysis of variance followed by Bonferroni's post hoc test. Statistical significance was set at $p < 0.05$.

■ ASSOCIATED CONTENT

Supporting Information

The Supporting Information is available free of charge on the ACS Publications website at DOI: 10.1021/acs.jmedchem.5b01521.

Example of a Guinier plot of SANS data, used to calculate R_g (PDF)

■ AUTHOR INFORMATION

Corresponding Author

*Phone: 0044 (0) 292 074 3504. Fax: 0044 (0) 292 074 2442. E-mail: FergusonEL@cardiff.ac.uk.

Present Address

⊥J.L.R. North Wales Centre for Primary Care Research, Bangor University, Gwenfro Units 4−8, Wrexham Technology Park, Wrexham LL13 7YP, U.K.

Author Contributions

The manuscript was written through contributions of all authors. All authors have given approval to the final version of the manuscript.

Notes

The authors declare no competing financial interest.

■ ACKNOWLEDGMENTS

This work was supported by a research grant from the Medical Research Council (via the Severnside Alliance for Translational Research). The ILL and the Science and Technology Facilities Council (STFC) are gratefully acknowledged for provision of neutron beamtime and consumables support. This work benefited from SasView software, originally developed by the DANSE project under NSF Award DMR-0520547.

■ ABBREVIATIONS

CD, circular dichroism; CMS, colistimethate sodium; D_2O, deuterium oxide; EGF, epidermal growth factor; ELISA, enzyme-linked immunosorbent assay; HK-2, human kidney 2; K-SFM, keratinocyte-serum-free medium; LAL, *Limulus* amebocyte lysate; LPS, lipopolysaccharide; NMR, nuclear magnetic resonance; PBS, phosphate buffered saline; SANS, small-angle neutron scattering; TNFα, tumor necrosis factor alpha

■ REFERENCES

(1) Travis, J. Reviving the antibiotic miracle? *Science* **1994**, *264*, 360−362.

(2) Ferguson, E. L.; Azzopardi, E. A.; Roberts, J. L.; Walsh, T. R.; Thomas, D. W. Dextrin−colistin conjugates as a model bioresponsive treatment for multi-drug resistant bacterial infections. *Mol. Pharmaceutics* **2014**, *11*, 4437−4447.

(3) Azzopardi, E. A.; Ferguson, E. L.; Thomas, D. W. Development and validation of an *in vitro* pharmacokinetic/ pharmacodynamic model to test the antibacterial efficacy of nanoantibiotics. *Antimicrob. Agents Chemother.* **2015**, *59*, 1837−1843.

(4) Duncan, R.; Gilbert, H. R. P.; Carbajo, R. J.; Vicent, M. J. Polymer masked-unmasked protein therapy (PUMPT) 1. Bioresponsive dextrin-trypsin and -MSH conjugates designed for α-amylase activation. *Biomacromolecules* **2008**, *9*, 1146−1154.

(5) Davies, B.; Cohen, J. Endotoxin removal devices for the treatment of sepsis and septic shock. *Lancet Infect. Dis.* **2011**, *11*, 65−71.

(6) Labischinski, H.; Vorgel, E.; Uebach, W.; May, R. P.; Bradaczek, H. Architecture of bacterial lipid A in solution. A neutron small-angle scattering study. *Eur. J. Biochem.* **1990**, *190*, 359−363.

(7) Bergstrand, A.; Svanberg, C.; Langton, M.; Nyden, M. Aggregation behavior and size of lipopolysaccharide from *Escherichia coli* O55:B5. *Colloids Surf., B* **2006**, *53*, 9−14.

(8) Santos, N. C.; Silva, A. C.; Castanho, M. A.; Martins-Silva, J.; Saldanha, C. Evaluation of lipopolysaccharide aggregation by light scattering spectroscopy. *ChemBioChem* **2003**, *4*, 96−100.

(9) Pristovsek, P.; Kidric, J. Solution structure of polymyxins B and E and effect of binding to lipopolysaccharide: an NMR and molecular modeling study. *J. Med. Chem.* **1999**, *42*, 4604−4613.

(10) Ferguson, E. L.; De Luca, E.; Heenan, R. K.; King, S. M.; Griffiths, P. C. Time-resolved small-angle neutron scattering as a tool for studying controlled release from liposomes using polymer-enzyme conjugates. *Macromol. Rapid Commun.* **2010**, *31*, 1685−1690.

(11) Aurell, C. A.; Wistrom, A. O. Critical aggregation concentrations of Gram-negative bacterial lipopolysaccharides (LPS). *Biochem. Biophys. Res. Commun.* **1998**, *253*, 119−123.

(12) Ryder, M. P.; Wu, X.; McKelvey, G. R.; McGuire, J.; Schilke, K. F. Binding interactions of bacterial lipopolysaccharide and the cationic amphiphilic peptides polymyxin B and WLBU2. *Colloids Surf., B* **2014**, *120*, 81−87.

(13) Warren, H. S.; Kania, S. A.; Siber, G. R. Binding and neutralization of bacterial lipopolysaccharide by colistin nonapeptide. *Antimicrob. Agents Chemother.* **1985**, *28*, 107−112.

(14) Kastowsky, M.; Gutberlet, T.; Bradaczek, H. Molecular modelling of the three-dimensional structure and conformational flexibility of bacterial lipopolysaccharide. *J. Bacteriol.* **1992**, *174*, 4798−4806.

(15) Wallace, S. J.; Li, J.; Nation, R. L.; Prankerd, R. J.; Velkov, T.; Boyd, B. J. Self-assembly behavior of colistin and its prodrug colistin methanesulfonate: implications for solution stability and solubilization. *J. Phys. Chem. B* **2010**, *114*, 4836−4840.

(16) Velkov, T.; Thompson, P. E.; Nation, R. L.; Li, J. Structure-activity relationships of polymyxin antibiotics. *J. Med. Chem.* **2010**, *53*, 1898−1916.

(17) Wannachaiyasit, S.; Chanvorachote, P.; Nimmannit, U. A novel anti-HIV dextrin-zidovudine conjugate improving the pharmacokinetics of zidovudine in rats. *AAPS PharmSciTech* **2008**, *9*, 840−850.

(18) Ferguson, E. L.; Duncan, R. Dextrin-phospholipase A_2: synthesis and evaluation as a novel bioresponsive anticancer conjugate. *Biomacromolecules* **2009**, *10*, 1358−1364.

DOI: 10.1021/acs.jmedchem.5b01521
J. Med. Chem. 2016, 59, 647−654

(19) Davtyan, T. K.; Mkrtchyan, N. R.; Manukyan, H. M.; Avetisyan, S. A. Dexamethasone, colchicine and iodine-lithium-alpha-dextrin act differentially on the oxidative burst and endotoxin tolerance induction *in vitro* in patients with Behcet's disease. *Int. Immunopharmacol.* **2006**, *6*, 396−407.
(20) Davtyan, T. K.; Hakobyan, I. S.; Muradyan, R. E.; Hovhannisyan, H. G.; Gabrielyan, E. S. Evaluation of amino acids as mediators for the antibacterial activity of iodine-lithium-alpha-dextrin *in vitro* and *in vivo*. *J. Antimicrob. Chemother.* **2007**, *59*, 1114−1122.
(21) Lake, P.; DeLeo, J.; Cerasoli, F.; Logdberg, L.; Weetall, M.; Handley, D. Pharmacodynamic evaluation of the neutralization of endotoxin by PMX622 in mice. *Antimicrob. Agents Chemother.* **2004**, *48*, 2987−2992.
(22) Bucklin, S. E.; Lake, P.; Logdberg, L.; Morrison, D. C. Therapeutic efficacy of a polymyxin B-dextran 70 conjugate in experimental model of endotoxemia. *Antimicrob. Agents Chemother.* **1995**, *39*, 1462−1466.

DOI: 10.1021/acs.jmedchem.5b01521
J. Med. Chem. 2016, 59, 647−654